Dissecting the Roles of a Strictly Conserved Tyrosine in Substrate Recognition and Catalysis by Pseudouridine 55 Synthase†

Kulwadee Phannachet, Youssef Elias, and Raven H. Huang*

Department of Biochemistry, School of Molecular and Cellular Biology, University of Illinois at Urbana−Champaign, 600 South Mathews Avenue, Urbana, Illinois 61801

Received May 24, 2005; Revised Manuscript Received September 16, 2005

ABSTRACT: Sequence alignment of the TruA, TruB, RsuA, and RluA families of pseudouridine synthases (ΨS) identifies a strictly conserved aspartic acid, which has been shown to be the critical nucleophile for the ΨS-catalyzed formation of pseudouridine (Ψ). However, superposition of the representative structures from these four families of enzymes identifies two additional amino acids, a lysine or an arginine (K/R) and a tyrosine (Y), from a K/RxY motif that are structurally conserved in the active site. We have created a series of *Thermotoga maritima* and *Escherichia coli* pseudouridine 55 synthase (Ψ55S) mutants in which the conserved Y is mutated to other amino acids. A new crystal structure of the *T. maritima* Ψ55S Y67F mutant in complex with a 5FU-RNA at 2.4 Å resolution revealed formation of 5-fluoro-6-hydroxypseudouridine (5FhΨ), the same product previously seen in wild-type Ψ55S−5FU-RNA complex structures. HPLC analysis confirmed efficient formation of 5FhΨ by both Ψ55S Y67F and Y67L mutants but to a much lesser extent by the Y67A mutant when 5FU-RNA substrate was used. However, both HPLC analysis and a tritium release assay indicated that these mutants had no detectable enzymatic activity when the natural RNA substrate was used. The combined structural and mutational studies lead us to propose that the side chain of the conserved tyrosine in these four families of ΨS plays a dual role within the active site, maintaining the structural integrity of the active site through its hydrophobic phenyl ring and acting as a general base through its OH group for the proton abstraction required in the last step of ΨS-catalyzed formation of Ψ.

Among 101 modified nucleosides documented to date, pseudouridine (Ψ)[1] was the first one to be discovered. Reports of its existence and its structural characterization occurred about half a century ago (*1*−*4*). Because of this historical priority, as well as the fact that it is the most abundant modified nucleotide in RNA, Ψ was called "the fifth nucleotide" following the four primary nucleotides, A, C, G, and U. Immediately after its structural characterization, it was recognized that Ψ was formed through isomerization of the naturally occurring U in RNA. However, 3 decades passed before the cloning and characterization of the first pseudouridine synthase (ΨS) that catalyzes the isomerization of U to form Ψ (*5*).

Since its discovery, many ΨS enzymes have been identified and categorized into four families, named after the *Escherichia coli* enzymes, TruA, TruB, RsuA, and RluA (*5*−*8*). More recently, a representative of a fifth family of ΨS, TruD, was cloned and was shown to be distinct from the first four families of enzymes (*9*). Initial sequence alignment of the first four families of ΨS only identified a strictly conserved aspartic acid (Figure 1a) (*10*). Biochemical studies indicate that the conserved aspartic acid is critical for catalysis, acting as the nucleophile either for the detachment of the base (C1′ mechanism) or for the rotation of the base (C6 mechanism) (*11*, *12*). Subsequent structural comparison of these four families of enzymes indicates that the conserved aspartic acid identified through sequence alignment is also structurally conserved (Figure 1b) (*13*−*16*). Moreover, structural comparison also identified two additional amino

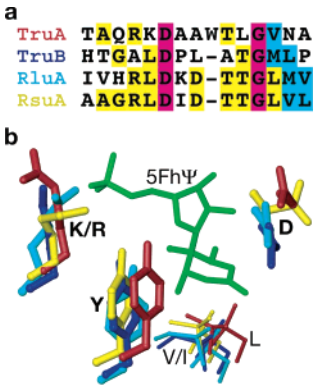

FIGURE 1: Sequence and structural alignments of four families of ΨS. (a) Sequence alignment of four families of ΨS. The conserved residues are boxed in color, with completely conserved residues in magenta, identical residues in yellow, and similar residues in cyan. (b) Superposition of representative structures from the four families of ΨS. Only the side chains of the conserved residues in the active site are shown and are colored accordingly to the labels in (a). The structure of 5FhΨ from the crystal structure of the TruB−RNA complex (PDB ID 1K8W) is shown in green to highlight the relative positions of the conserved residues in ΨS to the targeted nucleotide.

† This research was supported by NIH Grant CA90954.

* To whom correspondence should be addressed. Phone: (217) 333-3967. Fax: (217) 244-5858. E-mail: huang@uiuc.edu.

[1] Abbreviations: U, uridine; 5FU, 5-fluorouridine; Ψ, pseudouridine; 5FhΨ, 5-fluoro-6-hydroxypseudouridine; ΨS, pseudouridine synthase; Ψ55S, pseudouridine 55 synthase.

10.1021/bi050961w CCC: $30.25
Published on Web 11/03/2005

acids, a K/R and a Y within in a K/RxY motif (where x can be any amino acid) in all four families of enzymes, that are structurally conserved (Figure 1b).

Crystal structures of the TruB family of enzymes bound to 5FU-RNA revealed that the conserved K from the KxY motif forms a salt bridge with the phosphate of the targeted residue (Figure 1b) (*14*, *17*, *18*). Therefore, the role of the conserved K/R in the K/RxY motif is easy to understand: it interacts with the targeted nucleotide, possibly to secure its position for catalysis. On the other hand, understanding the possible roles of the strictly conserved Y in the K/RxY motif is less straightforward. Y is found to be part of the hydrophobic core in the active site, and its side chain is shown stacking against the targeted base (Figure 1b). Therefore, Y is likely to play a structural role in the architecture or the correct shape of the active site. However, if this were the only role it plays, then other hydrophobic residues, such as L, I, M, and especially F, would also be capable of carrying out the same structural role. The fact that no other amino acids other than Y are found in the K/RxY motif in the first four families of ΨS strongly suggests that Y has an additional role in ΨS catalysis.

To dissect the likely function of the conserved Y in the formation of Ψ catalyzed by ΨS, we have carried out structural and biochemical studies using wild-type Ψ55S and mutants in which the conserved Y was mutated to other amino acids. Here we report the crystal structure of the *Thermotoga maritima* Ψ55S Y67F mutant bound to a 5FU-RNA at 2.4 Å resolution. In addition to the Y-to-F mutation, we have also created other Y mutants and have carried out enzymatic assays of these mutants using both the natural and 5FU-RNA substrates. The findings from these studies allow us to propose the likely roles of the conserved Y in ΨS catalysis. The differences between TruD and the other four families of ΨS are also discussed.

MATERIALS AND METHODS

Creation, Overexpression, and Purification of the Conserved Tyrosine Mutants. Mutants of *T. maritima* and *E. coli* Ψ55S in which Y67 (*T. maritima*) or Y76 (*E. coli*) is replaced by other amino acids were generated using QuickChange site-directed mutagenesis kits (Stratagene). The previously constructed pLM-TM Ψ55S vector was used as the template for PCR (*18*). The procedures for overexpression and purification of the mutants were analogous to those of the wild-type enzymes previously reported (*18*).

Crystallization, Data Collection, Structural Determination, and Refinement. Crystallization of Y67F 5FU-RNA was performed using the hanging drop vapor diffusion method. Several RNA substrates originally used for crystallization screening of wild-type *T. maritima* Ψ55S were employed for initial crystallization trials with the Y67F mutant. In addition to crystals that were similar to those obtained for the wild-type enzyme, whose structure has been previously reported (*18*), a new thin plate crystal ($200 \times 100 \times 10$ μm^3) was obtained from a 5FU-RNA substrate that is one base pair shorter in the stem than the one for the wild-type structure. The new crystal grew in 2 weeks in a well solution containing 100 mM Tris-HCl, pH 8.5, 200 mM NaCl, and 15% PEG 6000, at 4 °C. Since the new crystals diffracted X-rays better than those in the same form as for the wild-type structure (2.4 vs 3.0 Å), structural determination of the Y67F mutant in complex with 5FU-RNA was based on the data collected from the new crystal. To carry out data collection at a low temperature, the crystals were briefly soaked in a cryoprotecting solution containing all of the components of the well solution plus 20% glycerol, mounted in a nylon loop, and then flash-frozen in liquid nitrogen. The data were collected at the 14-BMC beamline at the Advanced Photon Source (APS). Data were reduced with Denzo and Scalepack (*19*). The previously published structure of wild-type Ψ55S in complex with 5FU-RNA was used for molecular replacement calculations with AMoRe (*20*). To avoid bias, Y67 was changed to alanine and RNA was omitted in the starting search model. A few rounds of manual building using program O (*21*), followed by refinement with program CNS (*22*), resulted in a final model with an *R*-factor of 22.2% ($R_{free} = 27.2\%$). Final refinement statistics are given in Table 1.

Table 1: Statistics of Data Collection and Refinement

	Ψ55S(Y67F)−RNA complex
crystal	
space group	*P*21212
unit cell	157.83, 51.87, 57.15 90.00, 90.00, 90.00
resolution (Å)	50−2.4
wavelength (Å)	0.9792
unique reflections	19154
completeness (%)	99.7
average $I/\sigma(I)$[a]	10.8
redundancy	6.8
R_{sym}[b] (%)	5.6
refinement	
resolution (Å)	50−2.4
reflections (free)	15105 (1306)
$R_{crystal}$[c] (R_{free})[d] (%)	22.2 (27.2)
rmsd bonds (Å)	0.0062
rmsd angles (deg)	1.34

[a] $I/\sigma(I)$ is the mean reflection intensity/estimated error. [b] $R_{sym} = \sum|I - \langle I\rangle|/\sum I$, where I is the intensity of an individual reflection and $\langle I\rangle$ is the average intensity over symmetry equivalents. [c] $R_{crystal} = \sum||F_o| - |F_c||/\sum|F_o|$, where F_o and F_c are the observed and calculated structure factor amplitudes. [d] R_{free} is equivalent to $R_{crystal}$ but calculated for a randomly chosen set of reflections that were omitted from the refinement process.

HPLC Analysis of Formation of 5FhΨ and Ψ. The HPLC system was purchased from Waters (Waters 1525 binary HPLC pumps and Waters 2487 dual λ absorbance detector). A typical reaction (40 μL) for the analysis of formation of 5FhΨ from 5FU-RNA contained 0.5 μM Ψ55S (wild-type or mutants) and 5 μM 5FU-RNA in 10 mM HEPES, pH 7.0, 100 mM NaCl, and 1 mM DTT. After the samples were incubated at 37 °C for 3 h, the RNA products were digested with nuclease P1 (US Biological) with incubation at 37 °C for 10 min. The resulting nucleotides were dephosphorylated with shrimp alkaline phosphatase (SAP; Roche) at 37 °C for 10 min. The nucleosides were then separated by a SUPELCOSIL LC-18-S column (Supelco) with UV detection at 254 nm. The column was equilibrated with buffer A (20 mM NH_4OAc, pH 6.0), and nucleosides were eluted with gradient of buffer B (40% acetonitrile in water) using the following gradient: 0.0 min, 0% B; 3.0 min, 0% B; 10 min, 5% B; 21 min, 20% B; 22 min, 50% B; 25 min, 50% B; 26 min, 0% B; 35 min, 0% B, with constant flow rate of 2 mL/min.

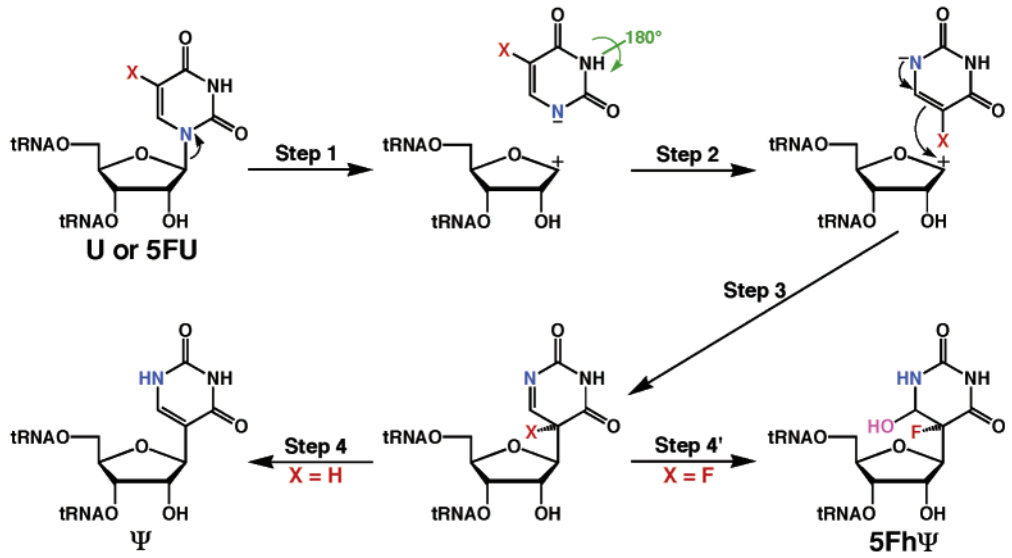

FIGURE 2: Steps required to convert U to Ψ or 5FU to 5FhΨ by Ψ55S. To form Ψ from U with the natural RNA substrate, or 5FhΨ from 5FU with 5FU-RNA, four steps are required. The first three, the breakage of glycosidic bond between the base and the ribose (step 1), the rotation of the detached base (step 2), and reattachment of the rotated base to the ribose through the C5 of the base (step 3), are shared by both U and 5FU. When X = H, the proton attached to the C5 is abstracted, resulting in formation of Ψ (step 4). When X = F, however, the F attached to the C5 remains. Instead, the double bond between the N1 and the C6 is hydrolyzed, resulting in formation of 5FhΨ.

Formation of Ψ from the natural RNA substrate was analyzed with the same protocol used for analysis of formation of 5FhΨ. For the reaction involving the wild-type enzyme, the concentration of enzyme was 0.05 μM, and the incubation time was 3 min. For Ψ55S Y67F, Y67L, and Y67A mutants, the concentration of the enzyme was increased to 5 μM (a 100-fold increase from wild type), and the incubation time was increased to 3 h (a 60-fold increase). For mass spectrometry, the peaks corresponding to 5FU, 5FhΨ, or Ψ were collected, concentrated, and subjected to electrospray ionization (ESI) mass spectrometry performed at the Mass Spectrometry Laboratory, School of Chemical Sciences, University of Illinois at Urbana−Champaign.

Tritium Release Assay. Our method was adopted from a reported procedure with slight modification (*23*). A sample (120 μL) containing a mixture of [5-^{3}H]Ura-RNA and unlabeled RNA (1:10 ratio, final concentration 4.62 μM) in TNE buffer (20 mM Tris-HCl, pH 8.0, 0.1 M NH_4Cl, 2 mM EDTA) was incubated at 37 °C for 2 min. Ψ55S (final concentration of 2 nM) was added to initiate the reaction. Aliquots of 18 μL were removed periodically (after 1−45 min), and the reaction was quenched by addition of 1 mL of 8% (w/v) Norit A in 0.1 M HCl. The mixtures were centrifuged at 15000 rpm for 10 min. The supernatants were filtered through glass wool. The pellets were resuspended with 0.5 mL of 8% (w/v) Norit A in 0.1 M HCl and centrifuged at 15000 rpm for 10 min. Supernatants were combined, and 10 mL of EcoscintA scintillation fluid (National Diagnostic) was added. ^{3}H released from the reaction was measured with a scintillation counter (model LS6500; Beckman Coulter). The enzymatic activities of Ψ55S mutants were determined by the same procedure except the final concentration of each mutant was 2 μM instead of 2 nM for the wild type (a 1000-fold increase).

RESULTS AND DISCUSSION

Steps Required To Convert U to Ψ or 5FU to 5FhΨ Catalyzed by Ψ55S. From a chemical point of view, four distinct steps are required to convert U to Ψ: (i) detachment of the U base, (ii) rotation of the detached U base to align C5 of the base to the C1′ of the ribose, (iii) reattachment of the rotated base through the formation of the C5−C1′ bond, and (iv) release of the proton attached to the C5 to form the final product Ψ (Figure 2). The crystal structures of the Ψ55S−5FU-RNA complex reported by us (*18*), as well as by others (*14*, *17*), revealed the formation of the 5FhΨ. Therefore, the targeted 5FU must have experienced the same first three steps of reaction as the natural substrate U, specifically, the detachment of the base, the rotation of the detached base, and reattachment of the rotated base through the C5 (Figure 2). However, since 5FU contains fluorine atom attached to the C5 (instead of the proton of the natural substrate, U), the release of F in order to form Ψ does not occur due to a very strong F−C bond. Instead, the double bond between N1 and C6 is hydrolyzed, resulting in formation of 5FhΨ (Figure 2, step 4′). Therefore, the Ψ55S-catalyzed reaction with the natural RNA substrate and 5FU-RNA shares the same first three steps of the reaction but differs in the last step. Hence, by studying the enzymatic reaction of the wild-type and mutated enzymes using both the natural substrate and 5FU-RNA, it is possible to decouple the final step of the reaction (release of the proton) from the first three steps. This enables us to identify any amino acids that are responsible only for the last step of the reaction, release of the proton attached to C5 in the formation of Ψ.

Structure of the Ψ55S Y67F Mutant Bound to a 5FU-RNA. Crystallization trials of the *T. maritima* Ψ55S Y67F mutant in a complex with a 5FU-RNA were carried out analogously to the wild-type enzyme (*18*). In contrast to the wild-type enzyme, which only produced crystals from one RNA construct, the Y67F mutant also yielded crystals from a second RNA construct that was one base pair shorter in the stem region. Furthermore, the new crystals diffracted X-rays better, and the structure of the Y67F mutant in a complex with a 5FU-RNA reported here was based on the data from the new crystal, with the final resolution of 2.4 Å

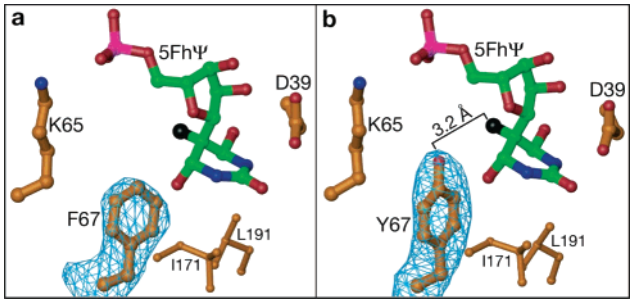

FIGURE 3: Structural comparison of the Ψ55S Y67F mutant (2.4 Å) with the wild-type enzyme (3.0 Å), both in complex with a 5FU-RNA. (a) Active site of the Ψ55S Y67F mutant with the simulated annealing $F_o - F_c$ omit map for residue F67. The 5FhΨ in RNA is colored green, and the side chains of Ψ55S are colored orange, with the heteroatoms in individual colors (nitrogen, blue; oxygen, red; phosphate, magenta; fluorine, black). (b) Active site of the wild-type Ψ55S (PDB ID 1ZU1). The figure is presented the same as in (a). The maps in both (a) and (b) are contoured at 5.0σ.

(compared to 3.0 Å for the wild type). The overall structure of the Y67F mutant complex was very similar to the complex with the wild-type enzyme, with an rmsd of 0.7 Å. However, they differed in crystal packing. While the crystals of the wild-type complex in our structure (*18*), as well as two other published structures (*14*, *17*), involve end-to-end stacking of the second RNA from a different complex, the RNA in the complex with the Y67F mutant in our new structure is free of other RNA contacts (data not shown). Therefore, this is the first crystal structure of Ψ55S in a complex with a stem-loop RNA, where a stem-loop RNA alone is sufficient for the formation of RNA product as well as crystal packing.

The structure of the Y67F mutant active site clearly shows the formation of 5FhΨ (Figure 3a), the same product observed in the previous structure of the wild-type enzyme (Figure 3b). The conformations of amino acids surrounding the 5FhΨ are virtually unchanged with the exception of the amino acid that is mutated, F67. The OH group in the side chain of Y67 in the wild-type structure is clearly missing in the structure of the Y67F mutant, as evidenced by the omit maps shown in Figure 3. In addition to the missing OH group, the conformation of the side chain of the mutated F67 is also slightly changed, with the phenyl ring moved closer to 5FhΨ, compared to Y67 in the wild-type structure (Figure 3). The difference likely results from the missing OH group because the steric restriction of the OH group in Y67 is absent in F67. Overall, our new structure clearly shows that, when 5FU-RNA is the substrate, the Y67F mutant behaves the same as the wild-type enzyme, capable of converting 5FU to 5FhΨ. HPLC analysis of reaction products of 5FU-RNA, discussed below, provides further evidence for this conclusion.

Enzymatic Activities of the Wild-Type Ψ55S and the Ψ55S Y76 Mutants (E. coli). The main method employed to determine the enzymatic activity of Ψ55S is HPLC analysis of the enzymatically digested product of Ψ55S-treated RNA substrates. The reason for choosing a HPLC system as our primary analysis tool is that HPLC allows us to analyze the reaction products using both the natural and the 5FU-RNA substrate. The disadvantage of HPLC analysis, when compared to a method using a radiolabeled substrate, is its sensitivity. Therefore, for the enzymatic assays using the

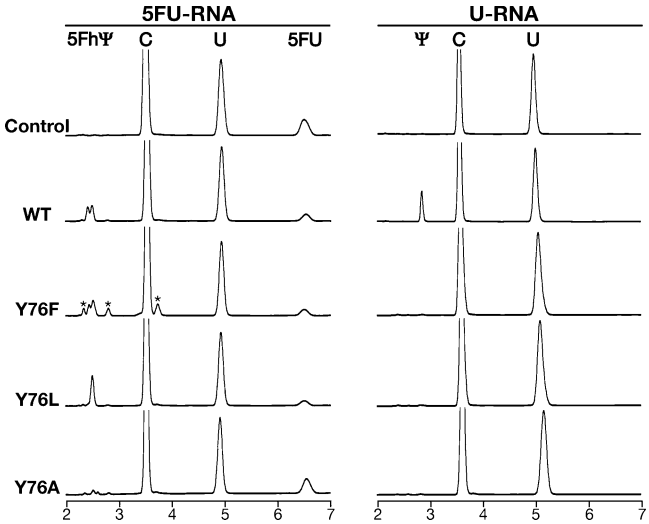

FIGURE 4: HPLC analysis of reaction products of 5FU-RNA (left panel) and natural RNA (right panel) incubated with *E. coli* Ψ55S wild-type or Y76 mutants. Only the region covering 5FhΨ, Ψ, C, U, and 5FU (retention time 2−7 min) is shown. Each stem-loop RNA was incubated with different enzymes, and the resulting RNA was enzymatically digested into nucleosides and analyzed by HPLC with a reverse-phase C18 column. Key: top panel, RNAs alone; second panel, RNAs + wild-type Ψ55S; third panel, RNAs + Ψ55S Y76F mutant; fourth panel, RNAs + Ψ55S Y76L mutant; bottom panel, RNAs + Ψ55S Y76A mutant. Although also observed in other panels, the impurity peaks marked by asterisks are much more pronounced in the left Y76F panel.

natural RNA substrate, a tritium release assay, commonly used in biochemical studies of ΨS-catalyzed reactions by other laboratories, was also carried out to confirm our HPLC results.

As we have reported previously, *T. maritima* Ψ55S forms a tightly bound complex with 5FU-RNA, mainly because of 5FhΨ formation (*18*). This was advantageous to our previous structural study but became a disadvantage for HPLC analysis because the RNA had to be separated from the enzyme before enzymatic digestion and HPLC analysis. Therefore, we employed *E. coli* Ψ55S for this study. The equivalent to Y67 in *T. maritima* Ψ55S is Y76 in the *E. coli* enzyme. HPLC analysis of the product of enzymatic digestion of 5FU-RNA alone resulted in a new peak with a retention time of 6.7 min, in addition to C, U, G, and A (Figure 4, top panel on left; peaks for G and A are omitted because of space). The identity of this peak as 5FU was confirmed by mass spectrometry (data not shown). HPLC analysis of the 5FU-RNA product after incubation with wild-type Ψ55S resulted in reduction of the 5FU peak and appearance of twin peaks with retention times of 2.5 and 2.6 min, respectively (Figure 4, second panel on left). The identity of the twin peaks as 5FhΨ was also confirmed by mass spectrometry (data not shown). This result is also consistent with the similar observation by Mueller and coworkers (*24*), suggesting that the twin peaks are cis and trans isomers of 5FhΨ. The cause of the residual 5FU peak is unknown, but it is possible that the enzyme is too sluggish with the 5FU-RNA substrate to convert all 5FU to 5FhΨ. Alternatively, a certain percentage of 5FU-RNA may not form a stem−loop (for example, in duplex form) and therefore cannot be recognized as a substrate by Ψ55S. When the wild-type Ψ55S was replaced by the Y76F mutant, the same change was observed, i.e., reduction of the peak

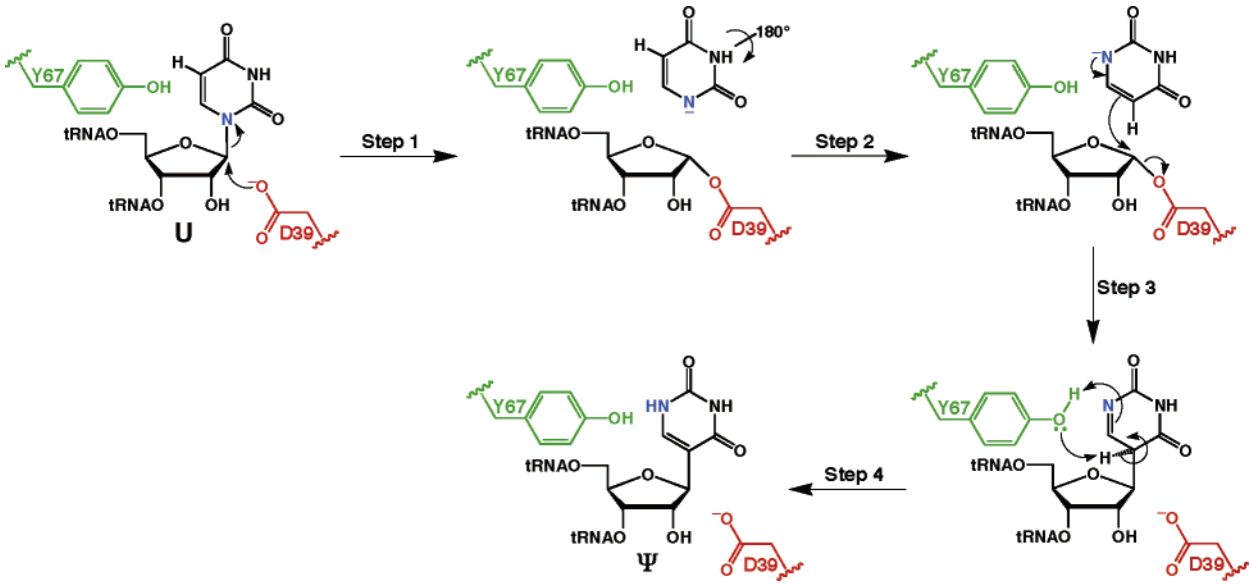

FIGURE 5: Proposed mechanism of Ψ formation by Ψ55S. The conserved aspartic acid is likely to be the nucleophile for the detachment of the base, and the conserved tyrosine is proposed to be the general base for the abstraction of the proton attached to the C5 of the base in the final step of the reaction to form the product Ψ.

corresponding to 5FU and appearance of twin peaks corresponding to 5FhΨ (Figure 4, the third panel on left). The additional small peaks marked by asterisks, which are also observed in other panels, are much more pronounced in this panel. The source of these impurity peaks is unknown, but the possibility that they are the reaction products of 5FU can be ruled out on the basis of the integration of the peak areas of 5FU and 5FhΨ, both in this panel as well as in the WT and Y76L panels. The formation of 5FhΨ as analyzed by HPLC is consistent with the crystal structure of the *T. maritima* Ψ55S Y67F mutant bound to 5FU-RNA as previously described. Similar results were obtained with the Y76L mutant (Figure 4, the fourth panel on left), but in this case, one of the twin peaks was dominant. Again, the identity of this predominant peak as 5FhΨ was confirmed by mass spectrometry (data not shown). Mutation of Y76 to A resulted in a substantial decrease in product yield, i.e., the twin peaks at 2.5 and 2.6 min (Figure 4, the bottom panel on left), indicating that a large hydrophobic side chain is important for 5FU-to-5FhΨ conversion. These experiments indicate that the wild-type enzyme and mutants Y76F and Y76L, but to a much lesser extent Y76A, are capable of converting 5FU into the 5FhΨ.

It is interesting to notice that the ratio of twin peaks of 5FhΨ changes from roughly equal with the WT enzyme, to one as majority with Y76F mutant, and to one dominating with Y76L mutant (Figure 4, left panels). In addition, only one isomer was observed in the structures (Figure 3). The possibility that only one isomer is formed enzymatically and it is later isomerized to the other in solution after dissociation of RNA from the enzyme can be ruled out because it would have produced the same results of the Y76F and Y76L mutants as the WT enzyme. It is possible that part of the hydrolysis is carried out without direct assistance of the enzyme, and the extent of nonenzymatic hydrolysis is lesser with the Y76F and Y76L mutants. Alternatively, all the hydrolysis can be carried out without direct assistance of the enzyme. The water is somehow able to access both sides of the C6 of 5FΨ to produce two isomers with a roughly equal amount in the presence of the WT enzyme, while the water is only able to access one side of 5FΨ when the Y76L mutant is bound. Since the only information relevant to dissecting the mechanism of ΨS-catalyzed reaction is whether a Ψ55S mutant is able to carry out the first three steps of the reaction shown in Figure 2 with 5FU-RNA as the substrate, we decided not to pursue further in terms of the likely mechanism of hydrolysis of 5FΨ to 5FhΨ.

When the natural RNA substrate was used, however, only the wild-type Ψ55S produced Ψ (Figure 4, the peak with the retention time of 3.4 min in the second panel on the right). The identity of this new peak as Ψ was confirmed by co-injection with authentic Ψ as well as mass spectrometry (data not shown). No Ψ peak was observed with Y76F, Y76L, and Y76A mutants (Figure 4, the bottom three panels on the right). Considering that the concentration of these mutants is 100-fold more than the wild type, and the reaction time is increased 60-fold relative to the wild type, it is reasonable to conclude that these mutations abolish the enzymatic activity of Ψ55S.

The more sensitive tritium release assay confirmed this conclusion from HPLC analysis. In our experiments, the k_{cat} and K_m of the wild-type Ψ55S are 0.18 ± 0.001 s^{-1} and 0.87 ± 0.16 μM, respectively, values comparable to those reported by Santi and co-workers (*23*). However, no enzymatic activity of Ψ55S Y76 mutants (Y76F, Y76L, and Y76A) was detected, despite a 1000-fold increase in enzyme concentration for the mutants (data not shown).

Proposed Mechanism. The structure of the Ψ55S Y67F mutant in complex with 5FU-RNA, together with our HPLC analysis of reaction products with 5FU-RNA as substrate, indicates that mutation of the strictly conserved Y67 (Y76 in *E. coli* enzyme) to F and L retains the enzyme's ability to convert 5FU to 5FhΨ. This conversion requires detachment, rotation, and reattachment of the base (Figure 2). If we assume that the enzyme behaves the same with 5FU-RNA as with the natural RNA substrate for the first three steps of the reaction, then Y67F and Y67L mutations do not affect the enzyme's ability to carry out the first three steps

of the natural enzymatic reaction. However, our HPLC analysis and tritium release assay indicate that these mutants are not active with the natural RNA substrate. Therefore, the conserved Y, specifically the OH group in the side chain of Y (the only difference between Y and F), must play a critical role in the final step of the reaction, which is the release of the proton from the C5 of the base. Taking into account all available data, we propose a likely mechanism of the Ψ55S-catalyzed reaction, as shown in Figure 5. Nucleophilic attack by the strictly conserved D39 on the C1′ of the ribose detaches the uracil base from the ribose (Figure 5, step 1). Rotation of the detached base and reattachment of the rotated base result in formation of the C5−C1′ bond between the base and the ribose (Figure 5, steps 2 and 3). The OH group of the strictly conserved Y67 abstracts the proton attached to C5 of the base (Figure 5, step 4).

Although it is generally agreed that the conserved aspartic acid (D39 in *T. maritima* Ψ55S) is critical for the enzymatic reaction of ΨS, its precise role is still in debate. Experimental evidence is available for supporting both a nucleophilic attack at the C1′ of the ribose, to assist the departure of the base (C1′ mechanism), and a nucleophilic attack at the C6 of the base, to assist the rotation of the base (C6 mechanism). With the recent report by Mueller and co-workers (*25*), as well as our own observations (*18*), the C1′ mechanism as presented in Figure 5 is preferred.

Final formation of Ψ requires not only release of the proton attached to C5 of the base but also gain of a proton at N1 of the base. It is possible that the side chain of Y67 donates its own proton to N1 of the base while abstracting the C5 proton as shown in Figure 5. In the crystal structure of wild-type Ψ55S in complex with a 5FU-RNA (*18*), the distance between the OH group of Y67 and N1 of 5FhΨ is 5.0 Å. One could image this distance would be shorter with the true intermediate because the OH group attached to C6 of the 5FhΨ would be absent in the true intermediate, making the proton transferring, depicted in Figure 5, possible. Alternatively, a nearby water molecule can act as a proton shuffle, accepting a proton from the side chain of the conserved tyrosine and donating a proton to N1 of the base. Formation of the hydrolyzed product 5FhΨ with 5FU-RNA as substrate indicates the accessibility of a water molecule to the active site.

The Exception of TruD. Since D39 and Y67 are also strictly conserved in the TruA, RsuA, and RluA families (Figure 1), the proposed mechanism shown in Figure 5 should also be applicable to these three families of ΨS. The only exception is the TruD family of enzymes. More recently, a fifth family of ΨS, TruD, was discovered (*9*), and the crystal structure of TruD has been reported by three groups (*26*−*28*). Superposition of TruD with the other four families of ΨS indicates the structural conservation of the critical aspartic acid. However, the structurally conserved tyrosine seen in the first four families of the enzyme is a phenylalanine in TruD (*26*−*28*). Sequence alignment of TruD homologues from bacteria, archaea, and eukarya (*9*), in combination with structural alignment, indicates that the equivalent of the K/RxY motif present in the first four families of ΨS is NxF in TruD, with strict conservation of both N and F. This raises the interesting possibility that TruD is mechanistically distinct from the other four families of ΨS, most likely in the final step of the reaction.

ACKNOWLEDGMENT

We thank the staff of beamline 14-BMC at APS (K. Brister, N. Lei, and R. Pahl) for support during data collection. We also thank C. Wraight for helpful discussions and critical reading of the manuscript.

REFERENCES

1. Cohn, W. E., and Volkin, E. (1951) Nucleoside-5′-phosphates from ribonucleic acid, *Nature 167*, 483−484.
2. Yu, C. T., and Allen, F. W. (1959) Studies on an isomer of uridine isolated from ribonucleic acids, *Biochim. Biophys. Acta 32*, 393−406.
3. Scannell, J. P., Crestfield, A. M., and Allen, F. W. (1959) Methylation studies on various uracil derivatives and on an isomer of uridine isolated from ribonucleic acids, *Biochim. Biophys. Acta 32*, 406−412.
4. Cohn, W. E. (1959) 5-Ribosyl uracil, a carbon−carbon ribofuranosyl nucleoside in ribonucleic acids, *Biochim. Biophys. Acta 32*, 569−571.
5. Kammen, H. O., Marvel, C. C., Hardy, L., and Penhoet, E. E. (1988) Purification, structure, and properties of *Escherichia coli* tRNA pseudouridine synthase I, *J. Biol. Chem. 263*, 2255−2263.
6. Nurse, K., Wrzesinski, J., Bakin, A., Lane, B. G., and Ofengand, J. (1995) Purification, cloning, and properties of the tRNA psi 55 synthase from *Escherichia coli*, *RNA 1*, 102−112.
7. Wrzesinski, J., Bakin, A., Nurse, K., Lane, B. G., and Ofengand, J. (1995) Purification, cloning, and properties of the 16S RNA pseudouridine 516 synthase from *Escherichia coli*, *Biochemistry 34*, 8904−8913.
8. Wrzesinski, J., Nurse, K., Bakin, A., Lane, B. G., and Ofengand, J. (1995) A dual-specificity pseudouridine synthase: an *Escherichia coli* synthase purified and cloned on the basis of its specificity for psi 746 in 23S RNA is also specific for psi 32 in tRNA(phe), *RNA 1*, 437−448.
9. Kaya, Y., and Ofengand, J. (2003) A novel unanticipated type of pseudouridine synthase with homologs in bacteria, archaea, and eukarya, *RNA 9*, 711−721.
10. Koonin, E. V. (1996) Pseudouridine synthases: four families of enzymes containing a putative uridine-binding motif also conserved in dUTPases and dCTP deaminases, *Nucleic Acids Res. 24*, 2411−2415.
11. Huang, L., Pookanjanatavip, M., Gu, X., and Santi, D. V. (1998) A conserved aspartate of tRNA pseudouridine synthase is essential for activity and a probable nucleophilic catalyst, *Biochemistry 37*, 344−351.
12. Gu, X., Liu, Y., and Santi, D. V. (1999) The mechanism of pseudouridine synthase I as deduced from its interaction with 5-fluorouracil-tRNA, *Proc. Natl. Acad. Sci. U.S.A. 96*, 14270−14275.
13. Foster, P. G., Huang, L., Santi, D. V., and Stroud, R. M. (2000) The structural basis for tRNA recognition and pseudouridine formation by pseudouridine synthase I, *Nat. Struct. Biol. 7*, 23−27.
14. Hoang, C., and Ferre-D'Amare, A. R. (2001) Cocrystal structure of a tRNA Psi55 pseudouridine synthase: nucleotide flipping by an RNA-modifying enzyme, *Cell 107*, 929−939.
15. Sivaraman, J., Sauve, V., Larocque, R., Stura, E. A., Schrag, J. D., Cygler, M., and Matte, A. (2002) Structure of the 16S rRNA pseudouridine synthase RsuA bound to uracil and UMP, *Nat. Struct. Biol. 9*, 353−358.
16. Sivaraman, J., Iannuzzi, P., Cygler, M., and Matte, A. (2004) Crystal structure of the RluD pseudouridine synthase catalytic module, an enzyme that modifies 23S rRNA and is essential for normal cell growth of *Escherichia coli*, *J. Mol. Biol. 335*, 87−101.
17. Pan, H., Agarwalla, S., Moustakas, D. T., Finer-Moore, J., and Stroud, R. M. (2003) Structure of tRNA pseudouridine synthase TruB and its RNA complex: RNA recognition through a combination of rigid docking and induced fit, *Proc. Natl. Acad. Sci. U.S.A. 100*, 12648−12653.
18. Phannachet, K., and Huang, R. H. (2004) Conformational change of pseudouridine 55 synthase upon its association with RNA substrate, *Nucleic Acids Res. 32*, 1422−1429.

19. Otwinowski, Z., and Minor, W. (1997) Processing of X-ray diffraction data collected in oscillation mode, in *Methods in Enzymology*, pp 307−326, Academic Press, San Diego, CA.
20. Navaza, J. (1994) AMoRe: an automated package for molecular replacement, *Acta Crystallogr. A50*, 157−163.
21. Jones, T. A., Zou, J.-Y., Cowan, S. W., and Kjeldgaard, M. (1991) Improved methods for building protein models in electron density maps and the location of errors in these models, *Acta Crystallogr. A47*, 110−119.
22. Brünger, A. T., Adams, P. D., Clore, G. M., DeLano, W. L., Gros, P., Grosse-Kunstleve, R. W., Jiang, J.-S., Kuszewski, J., Nilges, M., Pannu, N. S., Read, R. J., Rice, L. M., Simonson, T., and Warren, G. L. (1998) Crystallography & NMR system: A new software suite for macromolecular structure determination, *Acta Crystallogr. D54*, 905−921.
23. Gu, X., Yu, M., Ivanetich, K. M., and Santi, D. V. (1998) Molecular recognition of tRNA by tRNA pseudouridine 55 synthase, *Biochemistry 37*, 339−343.
24. Spedaliere, C. J., and Mueller, E. G. (2004) Not all pseudouridine synthases are potently inhibited by RNA containing 5-fluorouridine, *RNA 10*, 192−199.
25. Spedaliere, C. J., Ginter, J. M., Johnston, M. V., and Mueller, E. G. (2004) The pseudouridine synthases: revisiting a mechanism that seemed settled, *J. Am. Chem. Soc. 126*, 12758−12759.
26. Hoang, C., and Ferre-D'Amare, A. R. (2004) Crystal structure of the highly divergent pseudouridine synthase TruD reveals a circular permutation of a conserved fold, *RNA 10*, 1026−1033.
27. Kaya, Y., Del Campo, M., Ofengand, J., and Malhotra, A. (2004) Crystal structure of TruD, a novel pseudouridine synthase with a new protein fold, *J. Biol. Chem. 279*, 18107−18110.
28. Ericsson, U. B., Nordlund, P., and Hallberg, B. M. (2004) X-ray structure of tRNA pseudouridine synthase TruD reveals an inserted domain with a novel fold, *FEBS Lett. 565*, 59−64.

BI050961W